

Complete band gaps in three-dimensional quantum dot photonic crystals

Yong Zeng,^{1,2} Ying Fu,^{1,*} Xiaoshuang Chen,^{2,†} Wei Lu,^{2,‡} and Hans Ågren¹

¹*Department of Theoretical Chemistry, School of Biotechnology, Royal Institute of Technology, AlbaNova, S-106 91 Stockholm, Sweden*

²*National Laboratory for Infrared Physics, Shanghai Institute of Technical Physics, Chinese Academy of Science, 200083 Shanghai, China*

(Received 20 June 2006; revised manuscript received 11 August 2006; published 26 September 2006)

Nonlocal investigations have been performed about exciton-photon couplings in three-dimensional quantum-dot (QD) photonic crystals and a complete photonic band gap has been found in the band structure of a diamond lattice. The width of such a band gap can be broadened by increasing the filling ratio of the QDs (increasing the QD radius or/and decreasing the lattice constant of the photonic crystal). By decomposing the diamond lattice into two interlacing face-centered-cubic (fcc) sublattices, we have found that by significantly modifying the QD radius in one fcc sublattice (the diamond lattice therefore changed to the zinc blende lattice), the band structure of the zinc blende lattice is in principle the sum of two individual fcc sublattices. However, a huge exciton-photon coupling is observed near the band gaps of the two individual fcc sublattices when the radii of the QDs in the two fcc sublattices approach each other, resulting in the complete band gaps of the diamond structure.

DOI: 10.1103/PhysRevB.74.115325

PACS number(s): 73.63.Kv, 42.70.Qs, 41.20.-q

Starting from the pioneering papers of Yablonovich¹ and John² in 1987, the past two decades have witnessed a great deal of interest in photonic crystals (PCs), also named photonic band gap (PBG) materials. Conventional PCs consist of periodical dielectric arrays, which are normally referred to as passive PCs. One of their important properties is to mould and control the flow and distribution of the light at its most microscopic level. The synergetic interplay in these PCs between the microcavity resonances of composite particles and the Bragg scattering resonances of the dielectric arrays lead to the formation of a PBG, i.e., a range of frequencies for which no propagating electromagnetic (EM) modes are allowed. Due to the presence of the PBG in the dispersion relation of the EM field, the photonic density of states in PCs is suppressed in these band gaps.³ These features open the possibility for many important technological applications including lossless PC waveguides, low-threshold PC lasers, and high-Q PC nanocavities.⁴

Most of the early research efforts were concentrated on PBG materials consisting of positive and frequency-independent dielectrics. An assumption of frequency-independent dielectric constant implies the absence of internal excitations of the medium in a given frequency region. Under this condition, a scalar law can be used,⁴ that is, the PBG frequency is inversely proportional to the lattice constant. An interesting question has therefore arisen: what will happen when the size of the dielectric constituent is reduced to nanometer scale? Due to the quantum effects, clearly, the assumption that the dielectric permittivity is frequency independent is not valid anymore. As a consequence, many optical phenomena need to be restudied in the nanometer scale. For example, considering a three-dimensional (3D) PC consists of dielectric spheres fabricated using GaAs. The spheres are referred to as quantum dots (QDs) when their radii are reduced below 50 nm, and quantum confinement effects must be considered. Due to these quantum effects, a confined exciton can be optically excited in these QD materials by the propagating EM waves. When a photon and an exciton interact in the dispersion-crossover region, a combined quasiparticle, normally known as an exciton polariton, is formed.⁵

Because excitons in a macroscopic system spread through the whole structure with an appropriate dispersion, they must be treated with a nonlocal theory.^{6,7} Furthermore, the corresponding nonlocal dielectric polarization is given by

$$4\pi\mathbf{P}_{exc}(\mathbf{r}) = T(\omega) \left[\sum_a \Phi_a(\mathbf{r}) \int \Phi_a(\mathbf{r}') \mathbf{E}(\mathbf{r}') d\mathbf{r}' \right]. \quad (1)$$

Here, $\Phi_a(\mathbf{r})$ is the envelope function of the exciton excited in ath QD. Other terms are

$$T(\omega) = 2\pi \frac{\epsilon_b \omega_{LT} \omega_0 a_B^3}{\omega_0^2 - \omega^2}, \quad (2)$$

ω_{LT} and a_B are the exciton longitudinal-transverse splitting and Bohr radius in the corresponding bulk semiconductor, respectively. ϵ_b is the dielectric index of the well material. In order to emphasize the effect of the exciton polariton, here we neglect the tiny difference between dielectric indices of the well and barrier materials.⁸ This assumption is realistic for commonly used semiconductor materials such as III-V GaAs/Al_xGa_{1-x}As QDs. Denoting ω_0 as the ground-state exciton resonance frequency of QD whose radius is R , it is easy to obtain

$$\omega_0 = \frac{E_g}{\hbar} + \frac{\hbar \pi^2}{2m_0 R^2 e} \left(\frac{1}{m_e} + \frac{1}{m_h} \right), \quad (3)$$

when the QD is assumed as a spherical square quantum well. Here E_g is the band gap in the corresponding bulk semiconductor, e is the elementary charge, m_e and m_h are the electronic effective mass and hole effective mass, respectively.

Up to now, many investigations have been done in the field of optical properties of quantum dot based periodic structures. The effect of the exciton polariton in a one-dimensional photonic crystal was already studied,^{7,8} and a remarkable difference with the passive one was found, that is, PBG can exist even in the absence of a periodically modulated dielectric index.⁸ Many new interesting results concerning QD PCs have been obtained recently.⁹⁻¹⁴ On the

other hand, the photonic band structures of 3D QD PCs have been theoretically discussed by Fu and co-workers.¹⁵ However, a complete PBG has not been found in a face-centered-cubic (fcc) lattice, due to a symmetry-induced degeneracy at the W point, just as what happens in its passive counterpart.¹⁶ In this work, motivated by our recent work on nanospherical particle PCs (Ref. 17) and the important work presented in (Ref. 16) where a complete band gap is found in a diamond lattice consisting of passive dielectric sphere, we try to find a complete PBG in 3D semiconductor-QD (radii in the order of 20 nanometers) periodic structures, and a complete band gap is truly obtained when the QDs are arranged in a diamond lattice. It should be pointed out that, due to the fact that microstructured materials can manipulate electromagnetic radiation in the optical range, 3D QD periodic structures have many potential applications.^{10,17} For instance, an external radiation which excites the exciton in the QD will modify significantly the dielectric constant of the QD, i.e., the formation of an exciton polariton. This will change the photon density of states of the system, and cause many complex quantum-optics phenomena that affect the evolution of the excited QD and further modify the photon density of states again. The process iterates until dynamic equilibrium is achieved. Moreover, QD periodic structures can be used to fabricate active optical devices including a nanoscale optical waveguide.¹⁸

A diamond lattice consists of two interlacing fcc sublattices whose Brillouin zones are most spherelike, and it is favorable for the overlapping of band gaps at Brillouin-zone-boundary wave vectors.¹⁶ For the fcc Bravais lattice with a conventional cubic cell of size a , its reciprocal lattice is body-centered-cubic. Using the method developed in Refs. 15 and 17, the photonic band structures for a diamond lattice consisting of GaAs QDs along important symmetry lines in the Brillouin zone, $XU-UL-L\Gamma-\Gamma X-XW-WK$, are calculated and shown in Fig. 1. In the calculation, totally $19 \times 19 \times 19$ plane waves are used to achieve numerical convergence. The radius of QDs is assumed to be uniformly 20 nm, the lattice constant $a=115$ nm, the dielectric index of the well material $\epsilon_b=12.40$, the effective masses of electron and hole are $m_e=0.067$ and $m_h=0.51$, respectively, in the unit of electron rest mass, and the band gap is $E_g=1.519$ eV.¹⁹ It is clearly shown that a complete band gap exists between $[\omega_0 + 0.215\omega_{LT}, \omega_0 + 0.26\omega_{LT}]$. There are many interesting properties of the band structure of the QD PC:

(i) One profound similarity is found between our diamond QD structure and the diamond dielectric structure consisting of passive dielectric spheres.¹⁶ In both cases, all the bands along the symmetry line from X to W are twofold degenerate due to their symmetry. This favors the opening up of a gap between the lowest second and third bands which is what is required for a full photonic gap.

(ii) It is important to notice that the resonant wavelength λ_0 of a 20 nm GaAs QD is 1864.3284 nm, which is about 16 times the lattice constant a , which might suggest the long-wavelength approximation. In other words, the PC is effectively homogeneous for those propagating EM waves whose wavelengths are much longer than the lattice constant of PC. However, an approximately linear dispersion relationship cannot be allowed in our QD PC because of the strong dis-

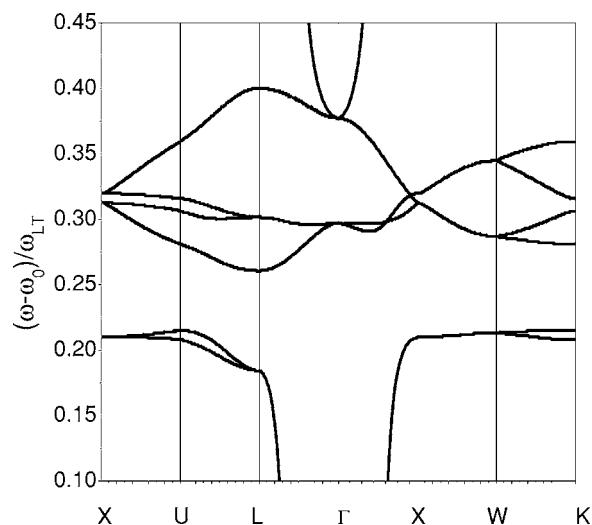


FIG. 1. Energy dispersion relation of a GaAs quantum dot diamond lattice. The following values are assumed for the numerical calculation: $a=115$ nm, $\hbar\omega_{LT}=0.5$ meV, and the radius of quantum dots $R=20$ nm. Here ω_0 ($\hbar\omega_0=1.535$ 01 eV) is the resonant frequency of the GaAs quantum dots.

persion around the band gap, and therefore, the PC cannot be approximated as an homogeneous material, and the long-wavelength approximation is not valid here.

(iii) The complete band gap exists in the region $[1864.1977, 1864.2311]$ nm, and its width is as small as 0.0334 nm, which is about 1.09×10^{-5} of the 20 nm QDs resonant wavelength λ_0 . Such a structure can be used to design a narrow-band omnidirectional reflector. Moreover, large variations appear in the spectrum of the density of photonic states because of the PBG structures, and strong enhancements of many quantum-optics phenomena, such as photon localization, spontaneous emission, and zero-point fluctuations, can be expected in our QD PC (Ref. 2).

The effect of the lattice constant a on the band gaps is shown in Fig. 2, where the width of the gap decreases with the increasing lattice constant. In a diamond lattice, a filling ratio, f , of the QD is normally defined as $f=8 \times 4\pi R^3/3a^3$. It is 26.8% when $a=100$ nm, and 12.2% when $a=130$ nm (the radius of the QD $R=20$ nm). Therefore, the width of the band gap increases with the filling ratio increasing from 12.2 to 26.8%. The result is in agreement with what happens in a diamond dielectric structure consisting of dielectric spheres.¹⁶ The photonic band structure as a function of radius of QDs is also studied in Fig. 3, and similar phenomenon appears. The lattice constant a is fixed at 100 nm, meanwhile the radius of QDs changes from 10 to 25 nm, corresponding to the filling ratio increase from 3.4 to 52.4%. Based on the above observation, we can therefore conclude that the width of the band gap can be increased by increasing the filling ratio of QDs in a diamond lattice. It is a consequence of the fact that the Bragg scattering resonances of the QD arrays will be enhanced with the increasing filling ratio.

It is already known that the introduction of a disorder into a perfect periodic structure will affect its band structure.⁴ We consider a special disorder in our QD diamond lattice by modifying the radius of the QDs in one fcc sublattice (in the

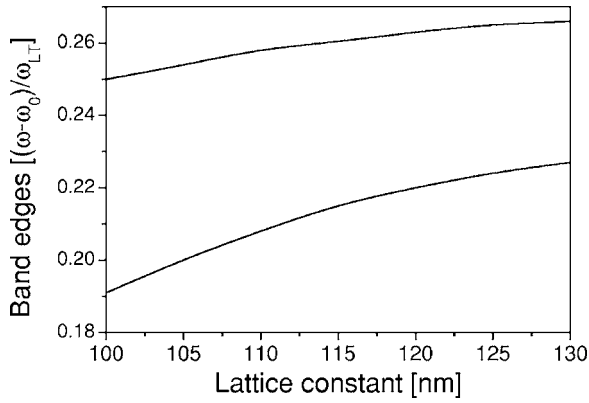


FIG. 2. The dependence of the band edges on the lattice constant a of a GaAs quantum dot diamond lattice. The following values are assumed for the numerical calculation: $\hbar\omega_{LT}=0.5$ meV and the radius of quantum dots $R=20$ nm. Here ω_0 ($\hbar\omega_0 = 1.535 01$ eV) is the resonant frequency of the GaAs quantum dots.

following, the modified fcc sublattice is referred to as a defective sublattice, and the corresponding QDs are referred to as defective QDs), so that the structure is changed from the diamond lattice to the zinc blende lattice. Notice that the resonant frequency of QDs, which is given by Eq. (3), is very sensitive to its radius when the radius is significantly small. In order to study this disordered structure, the methods presented in Ref. 17 are modified (see the Appendix for details) to take into account the difference of different-size QDs. The results are plotted in Fig. 4. Compared with the diamond lattice, the band structures of the zinc blende lattice are simpler, that is, degeneracies of the optical branches in general increase. In fact, the band structure of a zinc blende lattice is much like the one of a fcc lattice.^{15,17} Since the excitonic polarization is strong only in a very narrow frequency region around the resonant frequency of the QDs, the band structure of the zinc blende lattice shown in Fig. 4 is mainly decided by the unchanged QDs (here we just consider the frequency region around the resonant frequency of the unchanged QD). However, there is still one profound difference between the zinc blende and a fcc lattice. When the difference between two types of QDs is very small, there still

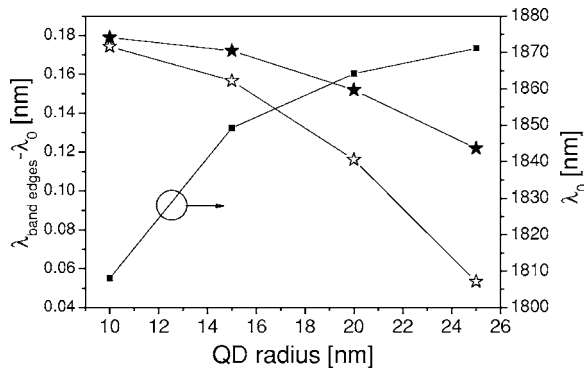


FIG. 3. The dependence of the band edges of a diamond lattice and the resonant wavelength λ_0 on the radius R of the GaAs QDs. The following values are assumed for the numerical calculation: $\hbar\omega_{LT}=0.5$ meV and the lattice constant $a=100$ nm. Here λ_0 is the resonant wavelength of the GaAs quantum dots.

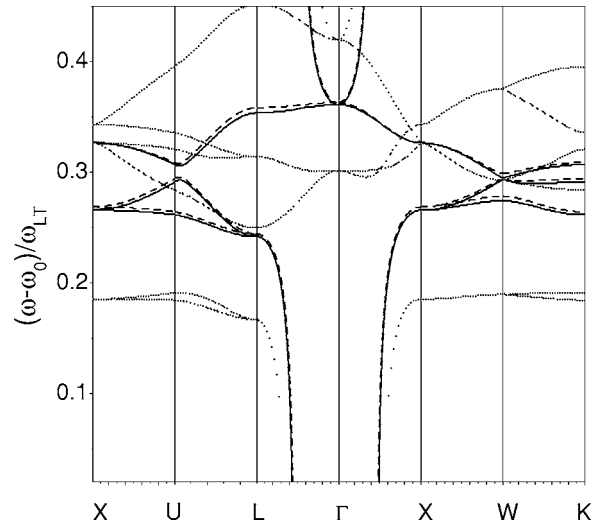


FIG. 4. Energy dispersion relations of two zinc blende structures consisting of two types of GaAs quantum dots whose radii are different. The following values are assumed for the numerical calculations: $a=100$ nm, $R_1=20$ nm, and $R_2=20.5$ nm (dashed); $a=100$ nm, $R_1=20$ nm, and $R_2=22$ nm (solid). In all cases, $\hbar\omega_{LT}=0.5$ meV, and $\hbar\omega_0=1.535 01$ eV (corresponding to the resonant frequency of the smaller GaAs quantum dot).

exists a gap between the second and the third band at the W point. Furthermore, when the radius of the defective QDs increases from 20.5 to 22 nm (the radius of the unchanged QDs is 20 nm), the gap disappears, in other words, the second and the third bands merge at the W point.

To elucidate the construction mechanism of the optical branches in Fig. 5, we plot the band structure of the zinc blende lattice when the defective QD radius is only 20.05 nm. A very interesting phenomenon is found: the lowest first, second, and third bands are very similar to the

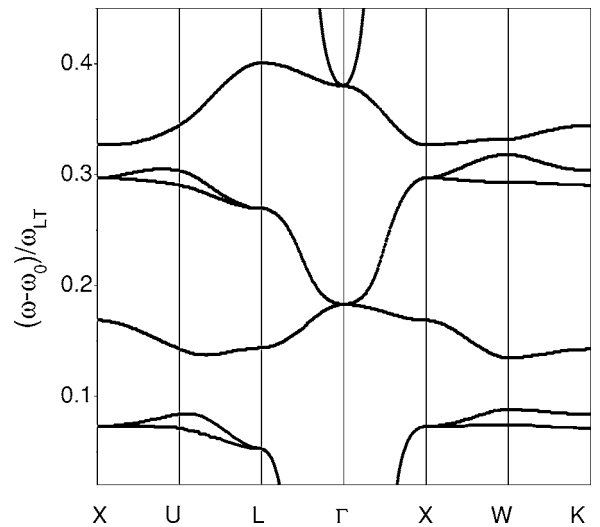


FIG. 5. Energy dispersion relations of one zinc blende structure consisting of two types of GaAs quantum dots whose radii are different. The following values are assumed for the numerical calculations: $a=100$ nm, $R_1=20$ nm, $R_2=20.05$ nm, $\hbar\omega_{LT}=0.5$ meV, and $\hbar\omega_0=1.535 01$ eV (corresponding to the resonant frequency of the smaller GaAs quantum dot).

fourth, fifth, and sixth bands. In fact, by calculating the band structures with the changing radius of the defective QD from 20.05 to 20.45, we can confirm that the lowest three bands belong to the defective fcc sublattice, and the fourth, fifth, and sixth bands belong to the unmodified fcc sublattice. In fact, with the increase of the radius of the defective QDs (so that the difference between the resonant frequencies of two types of QDs), the lowest three bands move downward, whereas only one set of the bands (fourth, fifth, and sixth) are left in the frequency window around ω_0 from the unchanged fcc lattice. In other words, when the radius of the defective QDs approaches that of the unmodified QDs, strong couplings between optical modes in the two similar fcc sublattices occur, and a complete band gap therefore becomes constructed.

Coevorden *et al.* calculated the photonic band structure of 3D atomic lattices where the permeability, related to resonance frequency, was modeled by delta functions centered at the atomic sites, and a complete PBG was obtained in the fcc atomic lattices.²⁰ Due to the difference between the local dipole-approximation permeability of the atomic lattice and the nonlocal permeability of our excitonic QD lattice, a significant difference can be found in the photonic band structures of atomic and QD lattices. The complete PBG of the QD PC is only obtained from complicated diamond lattices; it is not present in simple structures including primitive cubic and fcc lattices.¹⁵

In summary, nonlocal investigations have been performed on exciton-photon couplings in three-dimensional quantum dot (QD) photonic crystals and a complete photonic band gap has been found in the band structure of a diamond lattice. The width of such a band gap can be broadened by increasing the filling ratio of the QDs (increasing the QD radius or/and decreasing the lattice constant of the photonic crystal). By decomposing the diamond lattice into two interlacing face-centered-cubic (fcc) sublattices, we have found that by significantly modifying the QD radius in one fcc

sublattice (the diamond lattice therefore changed to the zinc blende lattice), the band structure of the zinc blende lattice is in principle the sum of two individual fcc sublattices. However, a huge exciton-photon coupling is observed near the band gaps of the two individual fcc sublattices when the radii of the QDs in the two fcc sublattices approach each other, resulting in the complete band gap of the diamond structure.

We thank Jun Jiang of the Royal Institute of Technology for his invaluable help. This work is supported by the Swedish Strategic Research Council (SSF), Chinese National Key Research Special Fund, Chinese National Science Foundation (Grants Nos. 60576068 and 60476040), the Grand fund of Chinese National Science Foundation (Grant No. 10234040), and Key Fund of Shanghai Science and Technology Foundation (Grant No. 05DJ14003).

APPENDIX

We start from the Maxwell equations (without external charges and currents) and the nonlocal excitonic polarization of the quantum-dot photonic crystal (Refs. 15 and 17)

$$4\pi\mathbf{P}_{exc}(\mathbf{r}) = T(\omega_1) \sum_a \Phi_{1,a}(\mathbf{r}) \int \Phi_{1,a}(\mathbf{r}') \mathbf{E}(\mathbf{r}') d\mathbf{r}' + T(\omega_2) \sum_{a+\Delta a} \Phi_{2,a+\Delta a}(\mathbf{r}) \int \Phi_{2,a+\Delta a}(\mathbf{r}') \mathbf{E}(\mathbf{r}') d\mathbf{r}'. \quad (\text{A1})$$

Next we decompose the vector function $\mathbf{E}_q(\mathbf{r})$ in terms of the Bloch wave vectors \mathbf{q} in the first Brillouin zone and reciprocal lattice vectors \mathbf{g} as follows:

$$\mathbf{E}_q(\mathbf{r}) = \sum_{\mathbf{g}} e^{i(\mathbf{q}+\mathbf{g})\cdot\mathbf{r}} \mathbf{E}_{\mathbf{q}+\mathbf{g}}. \quad (\text{A2})$$

After a series of derivations, a 6×6 matrix is achieved

$$D_{6 \times 6} = \begin{pmatrix} 1 - R_{1,11} & -R_{1,12} & -R_{1,13} & -R_{2,11} & -R_{2,12} & -R_{2,13} \\ -R_{1,21} & 1 - R_{1,22} & -R_{1,23} & -R_{2,21} & -R_{2,22} & -R_{2,23} \\ -R_{1,31} & -R_{1,32} & 1 - R_{1,33} & -R_{2,31} & -R_{2,32} & -R_{2,33} \\ R_{3,11} & R_{3,12} & R_{3,13} & R_{4,11} - 1 & R_{4,12} & R_{4,13} \\ R_{3,21} & R_{3,22} & R_{3,23} & R_{4,21} & R_{4,22} - 1 & R_{4,23} \\ R_{3,31} & R_{3,32} & R_{3,33} & R_{4,31} & R_{4,32} & R_{4,33} - 1 \end{pmatrix}, \quad (\text{A3})$$

with

$$R_{1,\alpha\beta}(\Omega, \mathbf{k}) = \frac{16\omega_{LT}R_1^3}{\pi\nu_0} \frac{\omega^2\omega_1}{\omega^2 - \omega_1^2} \sigma_{11,\alpha\beta}(\Omega, \mathbf{k}),$$

$$R_{2,\alpha\beta}(\Omega, \mathbf{k}) = \frac{16\omega_{LT}(R_1R_2)^{3/2}}{\pi\nu_0} \frac{\omega^2\omega_2}{\omega^2 - \omega_2^2} \sigma_{12,\alpha\beta}(\Omega, \mathbf{k}),$$

$$R_{3,\alpha\beta}(\Omega, \mathbf{k}) = \frac{16\omega_{LT}(R_1R_2)^{3/2}}{\pi\nu_0} \frac{\omega^2\omega_1}{\omega^2 - \omega_1^2} \sigma_{21,\alpha\beta}(\Omega, \mathbf{k}),$$

$$R_{4,\alpha\beta}(\Omega, \mathbf{k}) = \frac{16\omega_{LT}(R_2)^3}{\pi\nu_0} \frac{\omega^2\omega_2}{\omega^2 - \omega_2^2} \sigma_{22,\alpha\beta}(\Omega, \mathbf{k}), \quad (\text{A3}')$$

and

$$\sigma_{st,\alpha\beta}(\Omega, \mathbf{k}) = \sum_{\mathbf{b}} \frac{f(|\mathbf{b} + \mathbf{k}|R_s)f(|\mathbf{b} + \mathbf{k}|R_t)S_{\alpha\beta}(\mathbf{b} + \mathbf{k})}{\Omega^2 - \Omega^2(\mathbf{b} + \mathbf{k})} \times e^{i(s-t)(\mathbf{b}+\mathbf{k})\cdot\Delta\mathbf{a}},$$

$$f(x) = \frac{\pi^2 \sin x}{x(\pi^2 - x^2)},$$

$$\Omega = \omega,$$

$$\Omega(\mathbf{Q}) = \frac{c|\mathbf{Q}|}{n_b}, \quad (\text{A4})$$

where $\alpha, \beta = x, y, z$, and $s, t = 1, 2$. Finally, the dispersion law $\omega(\mathbf{q})$ can be obtained by solving

$$\text{Det}\|D\| = 0. \quad (\text{A5})$$

*Email address: fyg@theochem.kth.se

†Email address: xschen@mail.sitp.ac.cn

‡Email address: luwei@mail.sitp.ac.cn

¹E. Yablonovitch, Phys. Rev. Lett. **58**, 2059 (1987).

²S. John, Phys. Rev. Lett. **58**, 2486 (1987).

³Y. Zeng, X. S. Chen, and W. Lu, Phys. Rev. E **70**, 047601 (2004).

⁴K. Sakoda, *Optical Properties of Photonic Crystals* (Springer, Berlin, 2001).

⁵H. Haug and S. W. Koch, *Quantum Theory of the Optical and Electronic Properties of Semiconductors* (World Scientific, Singapore, 1986).

⁶R. Zeyher, J. L. Birman, and W. Brenig, Phys. Rev. B **6**, 4613 (1972).

⁷S. Nojima, Phys. Rev. B **59**, 5662 (1999).

⁸E. L. Ivchenko, M. M. Voronov, M. V. Erementschouk, L. I. Deych, and A. A. Lisyansky, Phys. Rev. B **70**, 195106 (2004).

⁹G. Ya. Slepyan, S. A. Maksimenko, V. P. Kalosha, A. Hoffmann, and D. Bimberg, Phys. Rev. B **64**, 125326 (2001).

¹⁰O. Voskoboynikov, C. M. J. Wijers, J. L. Liu, and C. P. Lee, Phys.

Rev. B **71**, 245332 (2005).

¹¹V. Bondarenko, M. Zaluzny, and Y. Zhao, Phys. Rev. B **71**, 115304 (2005).

¹²L. Belleguie and S. Mukamel, Phys. Rev. B **52**, 1936 (1995).

¹³F. Thiele, C. Fuchs, and R. v. Baltz, Phys. Rev. B **64**, 205309 (2001).

¹⁴X. Zhang and P. Sharma, Phys. Rev. B **72**, 195345 (2005).

¹⁵Y. Fu, M. Willander, and E. L. Ivchenko, Superlattices Microstruct. **27**, 255 (2000).

¹⁶K. M. Ho, C. T. Chan, and C. M. Soukoulis, Phys. Rev. Lett. **65**, 3152 (1990).

¹⁷Y. Zeng, X. Chen, W. Lu, and Y. Fu, Eur. Phys. J. B **49**, 313 (2006).

¹⁸Y. Fu, E. Berglind, L. Thylén, and H. Ågren (to be published).

¹⁹I. Vurgaftman, J. R. Meyer, and L. R. Ram-Mohan, J. Appl. Phys. **89**, 5815 (2001).

²⁰D. V. van Coevorden, R. Sprik, A. Tip, and A. Lagendijk, Phys. Rev. Lett. **77**, 2412 (1996).